Observation of a Raman-induced interpulse phase migration in the propagation of an ultrahigh-bit-rate coherent soliton train

Eric L. Buckland and Robert W. Boyd

The Institute of Optics, University of Rochester, Rochester, New York 14627

Alan F. Evans

Corning Incorporated, Sullivan Park, Corning, New York 14831

Received November 12, 1996

Coherent soliton packets generated in a passively mode-locked fiber laser are transmitted through 23 km of dispersion-decreasing fiber. We observe a shift of the phase difference between solitons that is due to intrapulse Raman scattering. We attribute the stability in propagation of these trains to a trade-off between minimizing soliton–soliton interactions by reduction of the pulse width and minimizing this Raman-induced phase migration, which can force the solitons into a deleterious attractive phase relationship. We are thus able to demonstrate the propagation of 177-Gbit/s soliton packets over a distance of 123 soliton periods.

Recently, ultrahigh-bit-rate transmission through optical fibers was demonstrated by use of highly multiplexed channels. For example, terabit-per-second transmission was achieved by means of multiplexing 55 discrete wavelength channels at 20 Gbits/s each, with a nonreturn-to-zero pulse format.[1] In a separate experiment, soliton time- and wavelength-division multiplexing were used to transmit eight 10-Gbit/s wavelength channels over a dispersion-managed link,[2] producing the highest bit-rate–distance product yet reported. Significant increases in the bit rate per wavelength channel are fundamentally inhibited by soliton–soliton interactions[3] and the Raman self-frequency shift.[4] In this Letter we demonstrate a unique stability region in the propagation of pulse trains as a function of the normalized pulse spacing. For closely spaced pulses, distortion-free propagation is inhibited by soliton–soliton interactions, whereas for well-separated but increasingly narrow pulses, the pulse train timing is destroyed by the influence of the Raman self-frequency shift. In the stability region soliton interactions are minimized, and we are able to demonstrate propagation of 177-Gbit/s coherent soliton packets through 23 km (greater than 100 soliton periods) of dispersion-decreasing fiber (DDF).

The source used in our experiments is a passively mode-locked figure-eight fiber laser[5] that forms a coherent packet of interacting solitons through a modulational instability, similar to behavior observed elsewhere.[6] A bandpass filter (bandwidth <5 nm) placed in the loop mirror provides tunability from 1540 to 1560 nm. The full-width pulse duration (T_{FWHM}) directly out of the laser is typically 1.25 ps, and the spectral width is 2.4 nm. The separation of pulses within the packet is 5.64 ps, for an effective intrapacket bit rate of $B = 177$ Gbits/s. A typical autocorrelation trace is shown in Fig. 1(a). The central peak is the autocorrelation signature of the individual pulses, whereas the outer peaks are the cross correlations of successively distant pulse pairs. The sharp triangular profile is indicative of excellent pulse-to-pulse amplitude stability, and the high visibility of the cross correlations suggests very low intrapacket timing jitter. The corresponding optical spectrum is shown in Fig. 1(b). The sharp spectral features are evidence of a high degree of coherence between pulses in the packet; the 1.40-nm spacing between spectral components is in agreement with the 177-Gbit/s repetition rate.

For the transmission experiments, the laser wavelength was tuned to 1541 nm in order to minimize the path-average dispersion of the test fiber. We adjusted the degree of interaction between solitons within a packet by narrowing the pulses through quasi-adiabatic amplification in an external erbium-doped fiber amplifier. By adjustment of the gain of the external amplifier, it was possible to maintain near-transform-limited pulses with normalized pulse separations $\sigma = 1/(BT_{\mathrm{FWHM}})$ ranging from 4 to 9.

The pulse trains were launched into a 23-km length of DDF designed to minimize the impact of fiber loss on pulse evolution.[5] The exponential dispersion decay coefficient of the DDF was $\alpha' = 0.0365\ \mathrm{km}^{-1}$, and the path-averaged dispersion was $\overline{D} = 1.75$ ps/(nm km). The power attenuation coeffi-

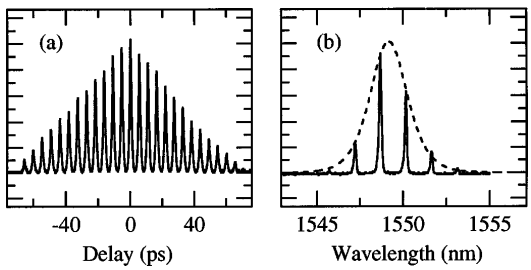

Fig. 1. (a) Intensity autocorrelation trace and (b) corresponding optical spectrum of a 13-soliton train. The dashed curve in (b) is the fit of the spectral peaks to a soliton envelope function of the form $\mathrm{sech}^2(\lambda - \lambda_0)$.

0146-9592/97/070454-03$10.00/0

cient α for the fiber was 0.0516 km^{-1}. In a previous experiment, isolated picosecond solitons from this figure-eight laser—operated in a mode that generated irregularly spaced, noninteracting solitons—were successfully transmitted without pulse broadening through a 40-km span of this DDF.[5] The soliton packets in the current experiment were less than 100 ps long, and separated by 260 ns, so that acoustic interactions were not important.[7,8] It was therefore expected that propagation dynamics in the current experiment would be dominated by short-range soliton–soliton interactions and the influence of the Raman self-frequency shift (RSFS).

At the output of the DDF, timing jitter within the pulse packets and the coherence of the optical spectra were strongly dependent on the normalized pulse spacing σ. Autocorrelation traces and spectra are shown in Fig. 2 for the packets with input spacings of $\sigma = 5.27$, $\sigma = 6.25$, and $\sigma = 7.05$. The pulse packets that were generated with the intermediate pulse spacings of $\sigma = 5.27$ and $\sigma = 6.25$ were transmitted through the DDF with a minimum of distortion; the autocorrelation traces show clearly resolved central peaks, and the cross correlations of all neighboring pulse pairs are resolved (for clarity only nearest-neighbor cross correlations are shown). The discrete nature of the spectra was preserved, indicating that the coherence of the pulse train was maintained, although some evidence of broadband noise in the Raman amplification process is visible in Fig. 2 as a broadening of the long-wavelength spectral components toward the blue. Conversely, timing information and spectral coherence of the pulse packets at both extremes of normalized pulse spacing were completely destroyed. No signature of a pulse train was recoverable at $\sigma = 4.70$; propagation dynamics of these closely spaced pulses were ostensibly dominated by short-range soliton–soliton interactions. At $\sigma = 7.05$, where soliton–soliton interactions were expected to be minimized, the intensity autocorrelation showed an identifiable pulse signature but the visibility of the cross correlations was reduced to zero. The spectrum shifted sharply toward the red and lost any sign of coherence.

The evolution of the spectra clearly demonstrates the increasing influence of intrapulse Raman scattering as the pulse widths are decreased. In DDF, the expected Raman wavelength shift after propagation of a distance L is given by[4,9]

$$d\lambda(L) = \frac{2\lambda^4 T_R}{15\pi^2 c^2 T_0^4}\overline{D}L, \qquad (1)$$

where λ is the soliton center wavelength, $\overline{D}$ is the path-averaged dispersion of the transmission fiber, and T_R is the effective Raman response time. In Fig. 3(a), the measured wavelength shift and the shift predicted by Eq. (1) are shown for the three input conditions that had an identifiable output signature. The shift in the center wavelength has the further effect of broadening pulses, even within DDF, because of the disruption in the balance between self-phase modulation and group-velocity dispersion that is due to the nonzero third-order dispersion. This pulse broadening can be expected to increase soliton–soliton interactions and reduce the effective collision length. This effect is not

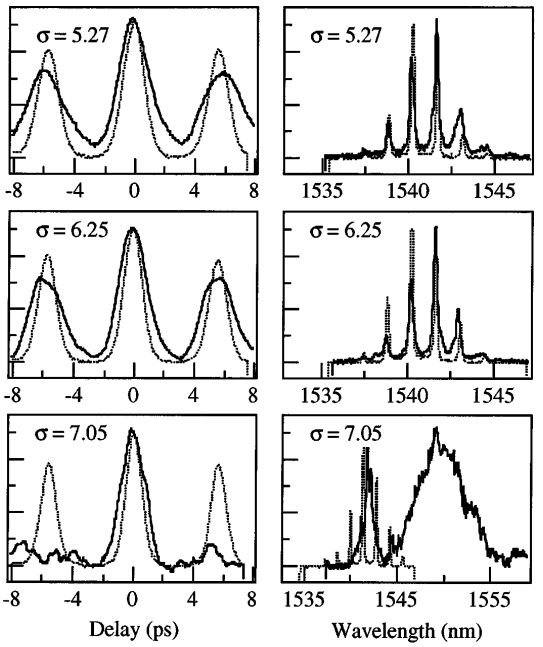

Fig. 2. Output autocorrelation traces (left) and spectra (right) for three values of the normalized pulse spacing σ. The solid curves refer to the output of the fiber; the dotted curves refer to the input. Note the change in horizontal scale for the spectrum associated with $\sigma = 7.05$.

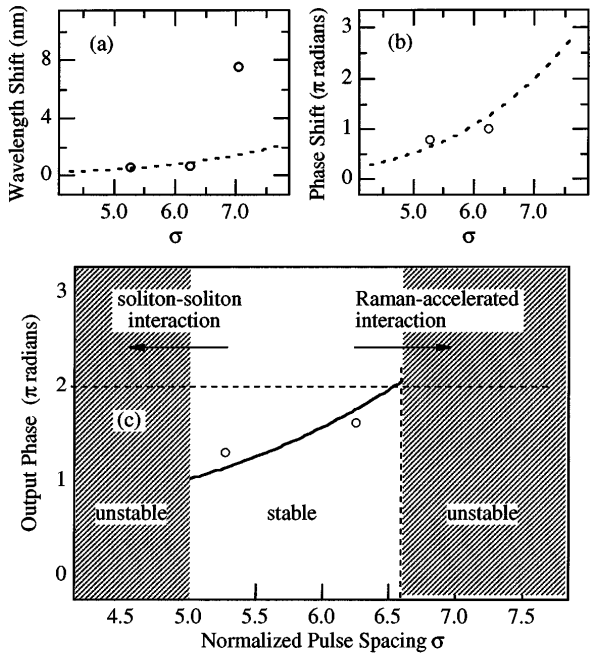

Fig. 3. (a) Wavelength shifts, (b) phase-difference shifts, and (c) output phase difference because of intrapulse Raman scattering. The dashed curves in (a) and (b) are predictions of Eqs. (1) and (4), respectively, assuming that $T_R = 2$ fs. The solid curve in (c) is the predicted intersoliton phase difference at the output when the input phase difference is $\pi/2$. The propagation limit is indicated by the dashed line in (c), at which point the intersoliton phase difference reaches 2π at the output of the 23-km fiber.

immediately evident for the recovered packets that had input pulse spacings of $\sigma = 5.27$ and $\sigma = 6.25$, because the shifts in the center wavelength are quite small.

Neither the Raman red shift, the associated pulse broadening, nor noise in the Raman amplification process is sufficient to explain the destruction of the pulse train observed when the normalized pulse spacing was increased to $\sigma = 7.05$. It is well known that during the collision of ultrashort solitons with a relative phase difference of 2π there is an acceleration of the self-frequency shift because of the increased energy localization.[10] The relative phase between solitons at the input to the test fiber was $\pi/2$, as discussed below, for all cases of the normalized pulse spacing σ; this implies a repulsive interaction between the solitons[11,12] that cannot explain the accelerated red shift seen in Fig. 2 for $\sigma = 7.05$. We surmise that the migration in the intersoliton phase difference associated with the RSFS, which can force the solitons to evolve into the attractive 2π state, is the critical factor limiting transmission of these interacting soliton packets as the pulse width is reduced.

The optical spectrum and the temporal envelope function for a soliton train are related by the Fourier transform pair:

$$|A(\nu - \nu_0)|^2 = (\pi T_0 B)^2 \operatorname{sech}^2\left[\pi^2 T_0(\nu - \nu_0)\right] \times \sum_m \delta[(\nu - \nu_0) - (m + f)B], \quad (2)$$

$$\tilde{A}(t) = \sum_n \operatorname{sech}\left(\frac{t - n/B}{T_0}\right)\exp(i2\pi f B t), \quad (3)$$

where ν_0 is the central frequency, T_0 is the soliton pulse width, B is the bit rate, f is the fractional shift of the peak spectral component from the center of the envelope, and the phase difference between adjacent solitons is $|2\pi f|$. As the Raman pumping shifts the mean frequency, it also changes the spectral asymmetry. This change in spectral asymmetry directly corresponds to a migration of the intersoliton phase difference, by an amount equal to $2\pi f$, where $f = d\lambda/\Delta\lambda$ is the wavelength shift as a fraction of the wavelength separation $\Delta\lambda = \lambda^2 B/c$. This change in the phase difference between successive solitons in the pulse train can be expressed by

$$d\phi(L) = \frac{4\lambda^2 T_R}{15\pi c}\left(\frac{\sigma T_{\mathrm{FWHM}}}{T_0}\right)^4 B^3 \overline{D} L. \quad (4)$$

The observed and the predicted shifts of the interpulse phase difference and the terminal values of the relative soliton phase at the output of the 23-km DDF are plotted in Figs. 3(b) and 3(c), respectively; no experimental result is plotted for $\sigma = 7.05$ in Figs. 3(b) and 3(c) because there is no phase information in the spectrum at the output of the DDF.

As shown in Fig. 3(c), only the pulse packet with an input pulse spacing of $\sigma = 7.05$ experienced a migration of the relative phase difference sufficient to force the solitons into an attractive 2π state. Although the reduced pulse width was expected to reduce soliton–soliton interactions,[3] feedback between an enhancement in the soliton–soliton interaction (caused by pulse broadening from the combined actions of the RSFS and third-order dispersion) and the acceleration of the RSFS during collision of the attractive solitons[10] may instead have reduced the effective collision distance. This accelerated soliton–soliton interaction brought on by the migration of the relative soliton phase may then explain the observed acceleration of the frequency shift, the destruction of the coherence of the pulse train, and the loss of the identity of individual pulses observed for the pulse packets with an input normalized pulse spacing of $\sigma = 7.05$.

In conclusion, we have demonstrated the propagation of interacting picosecond solitons over 123 soliton periods in 23 km of dispersion-decreasing fiber. We observe a migration of the intersoliton phase difference associated with the Raman self-frequency shift and attribute the stability in propagation of these pulse trains to a trade-off between minimizing soliton–soliton interactions and minimizing the Raman-induced phase migration, which can force the solitons into a deleterious attractive phase relationship. Further, we see that when the initial soliton phase difference is set to a minimum positive value, the solitons can tolerate a maximum phase migration and therefore have the potential to be stable over the longest propagation distances.

E. L. Buckland acknowledges support through a National Defense Science and Engineering Graduate Fellowship. This research was sponsored by the Center for Electronic Imaging Systems, University of Rochester, by the National Science Foundation, and by the U.S. Army Research Office.

References

1. A. R. Chraplyvy, A. H. Gnauck, R. W. Tkach, J. L. Zyskind, J. W. Sulhoff, A. J. Lucero, Y. Sun, R. M. Jopson, F. Foghieri, R. M. Derosier, C. Wolf, and A. R. McCormick, IEEE Photon. Technol. Lett. **8,** 1264 (1996).
2. L. F. Mollenauer, P. V. Mamyshev, and M. J. Neubelt, in *Optical Fiber Communication Conference*, Vol. 2 of 1996 OSA Technical Digest Series (Optical Society of America, Washington, D.C., 1996), paper PD22.
3. G. P. Agrawal, *Nonlinear Fiber Optics*, 2nd ed. (Academic, Boston, Mass., 1995).
4. J. P. Gordon, Opt. Lett. **11,** 662 (1986).
5. A. J. Stentz, R. W. Boyd, and A. F. Evans, Opt. Lett. **20,** 1770 (1995).
6. M. J. Guy, D. U. Noske, and J. R. Taylor, Opt. Lett. **18,** 1447 (1993).
7. E. M. Dianov, A. V. Luchnikov, A. N. Pilipetskii, and A. N. Starodumov, Opt. Lett. **15,** 314 (1990); E. M. Dianov, A. V. Luchnikov, A. N. Pilipetskii, and A. M. Prokhorov, Appl. Phys. B **54,** 175 (1992).
8. E. L. Buckland and R. W. Boyd, Opt. Lett. **21,** 1117 (1996).
9. R.-J. Essiambre and G. P. Agrawal, Opt. Lett. **21,** 116 (1996).
10. K. Kurokawa, H. Kubota, and M. Nakazawa, IEEE J. Quantum Electron. **30,** 2220 (1994).
11. F. M. Mitschke, Opt. Lett. **12,** 355 (1987).
12. Y. Kodama, Opt. Lett. **12,** 1038 (1987).